2022-11

On the use of constrained focused waves for characteristic load prediction

Tosdevin, Tom

On the use of constrained focused waves for characteristic load prediction

T. Tosdevin & S. Jin & D. Simmonds & M. Hann & D. Greaves
COAST research group
University of Plymouth, Plymouth, UK

ABSTRACT: Physical experiments investigating the extreme responses of a semi-submersible floating offshore wind turbine were conducted to allow a comparison of design wave methods. A 1:70 scale model of the IEA 15MW reference turbine and VolturnUS-S platform was studied focusing on the hydrodynamics under parked turbine conditions. A comparison of characteristic load predictions was made between design standard recommendations by the IEC and DNV covering different design wave types and post processing methods. Constrained waves are permitted for predicting characteristic loads for fixed offshore turbines but the extent to which they are suitable for floating devices is questionable. A constrained wave method for characteristic load prediction is applied and it is concluded that in general characteristic responses related to pitch may be estimated well with single response conditioned focused waves but for response types where the low frequency surge is important, e.g. mooring loads, constrained focused waves need to be applied.

1 INTRODUCTION

The fast and accurate prediction of design loads for floating offshore renewable energy (ORE) devices is an area of research which has the potential to improve the efficiency of the design process. Constrained wave methods which seek to reduce the simulation times required using multiple irregular wave time series consist of constraining a wave profile likely to produce a desired extreme response into a short random irregular background. Design standards for fixed offshore wind, such as IEC (2014) and DNV (2016) permit the use of the constrained wave method in the prediction of the characteristic loads/responses. The established method used in fixed offshore wind is to constrain a nonlinear regular or stream function wave (Rainey & Camp 2007). An identical approach cannot be applied to floating wind cases and is not recommended in the IEC standards (IEC 2019). Wave and tidal energy standards IEC (2016) and IEC (2015) permit the use of short design wave methods where it can be shown that they are at least as conservative as traditional irregular wave methods. It is unlikely for dynamic floating devices that a nonlinear regular wave will produce the extreme response of interest and so a response conditioned focused wave approach is adopted in this work. This paper investigates the application of a constrained wave method for a 1:70 scale model semi submersible floating wind turbine focusing on the mooring loads, pitch response and the x acceleration of the nacelle.

2 DESIGN STANDARDS AND CHARACTERISTIC LOAD PREDICTION

The contour method is a commonly applied design approach where an x year return contour, 50 years typically for ORE applications, is fitted to Hs, Tp hindcast data. A minimum of 20 years of data is recommended and the IFORM approach most commonly applied (DNV 2014a). The sea state along the contour producing the largest load / response of interest is then identified as the design sea and a characteristic load determined, the design load is then defined by multiplying by a safety factor.

Different standards recommend different methods for predicting the characteristic load. The two described here are the standards produced by the DNV and IEC. The approaches may be split into two categories, termed here the high percentile and average of maxima approaches. The high percentile method calculates the short term extreme value distribution (EVD) of the response of interest in the design sea state and selects a high percentile of the cumulative

distribution function (CDF) as the characteristic load. This percentile is determined from empirical observations for established offshore industries and will need to be refined for ORE applications once data becomes available. The percentile is reported as being in excess of 75% for offshore applications using a 100yr contour in DNV (2014b). A related but alternative approach to this would be to inflate the contour and select the 50th percentile as in Winterstein et al. (1993). The high percentile method is recommended in several DNV documents (DNV (2018),DNV (2014b)). The average of maxima approach runs multiple irregular wave time series each with a different random phase seed and the characteristic load/response is taken as the average of the maxima from each seed. Usually this is the mean but for mooring loads it is the most probable maximum (MPM) assuming a Gumbel distribution (DNV (2015), DNV (2018), IEC (2015)). Variants of this approach applied to other response types include taking the mean of the largest half of the maxima as in IEC (2014).

The post processing method applied here follows the average of maxima approach as it is recommended by both the IEC and DNV for moorings (DNV (2015), DNV (2018), IEC (2015)). Typically the mooring load is split into mean and dynamic components, the MPM of the dynamic mooring load assuming a Gumbel distribution is calculated and different safety factors applied to each component. In this work the mooring load is not split into components and the mean of the maxima is used instead of the MPM. This was done so as to facilitate a better comparison between response types and is appropriate as it has little effect on the comparison being drawn between the constrained and irregular wave methods.

3 FOCUSED WAVES

Focused waves have long been used to study extreme responses in offshore engineering. The NewWave produces the profile of the most likely largest wave for a particular sea state. Response conditioned focused waves such as the most likely extreme response (MLER) wave produce the profile of the wave most likely to induce an extreme response according to linear response amplitude operators (RAOs). These wave profiles must then be scaled to a particular target wave or response amplitude respectively which can be calculated from the wave or response spectra. However for some response types of dynamic, floating ORE it is found that single focused waves fail to produce extremes. Mooring loads in particular are a good example of this as often a certain amount of wave time series preceding the extreme event is necessary to produce a surge offset. To try to remedy this short coming, focused waves can be constrained into short irregular wave backgrounds, the constrained version of the MLER developed in Dietz (2005) is termed the conditional random response wave (CRRW). However previous applications of constrained focused waves (Tosdevin et al. 2021) have highlighted that history effects, deviations in the extreme amplitude distribution from linear wave theory and the physical error in reproducing specific wave time series, frustrate their straightforward application. Therefore a calibration procedure where a single phase correction is applied to the focused wave and then used for all subsequent constrained focused wave cases was suggested. The scaling of the focused waves to a high percentile of the linear EVD prediction, the 99th in Tosdevin et al. (2021) and this work, was also found to produce responses more in line with those produced by irregular waves. Detailed equations are not given here but for the response conditioned methods for ORE applications see Quon et al. (2016) for the MLER wave and Tosdevin et al. (2021) for the CRRW and MLER methods and how they can be appropriately scaled. The treatment of NewWaves can be found in many papers e.g. Tromans et al. (1991).

In summary, the procedure applied in this work was developed as part of work package 4 of the Supergen ORE Hub and consists of using response conditioned focused waves scaled to the 99th percentile of the linear response EVD prediction. A fast calibration is achieved by applying a phase correction to all constrained wave cases calculated from the single focused wave. The average of the responses produced is then taken to predict the characteristic load following the average of maxima post processing method most commonly applied in the IEC standards. It is hoped that the evidence presented in this and subsequent papers will aid ORE designers in determining when and how single and constrained focused waves may be used in the design process for characteristic load prediction.

4 MODEL AND SITE CONDITIONS

Experiments on the University of Maine's VolturnUS-S floating offshore wind platform and IEA 15MW reference turbine were conducted in the COAST lab's ocean basin at the University of Plymouth. This device benefits from extensive publicly available data including an OpenFAST model. It is moored with 3 catenary chains. The results presented here are for a single sea state under parked conditions. The model was constructed using the specifications for the reference device given in Allen et al. (2020). Table 1 gives a comparison of the target and achieved mass properties and the model is shown in figure 1. The draft of the model matches the full scale target of 20m. The model and probe locations are given in table 2.

The site of interest was taken as an intended deployment location for FOWTs off the coast of Maine on the east coast of the USA as described in Viselli et al. (2015). 30 years of hindcast data from the ECMWF (Hersbach et al. 2018) was used to fit a 50 year return period contour using mean wind speed

Table 1: Model details estimated from a solid works model from the lab technician, moments of inertia are taken about the centre of mass, vertical centre of gravity (VCG) is taken from the model base and the centre of gravity in x (XCG) from the tower centre.

Mass properties	Target	Achieved	Difference
$Ixx\ (kgm^2)$	26.495	26.550	0.055
$Iyy\ (kgm^2)$	26.451	26.551	0.099
$Izz\ (kgm^2)$	14.206	14.120	-0.086
$VCG\ (mm)$	255.14	261.57	6.43
$XCG\ (mm)$	4.28	0.48	-3.8
$Mass\ (kg)$	58.123	56.23	-1.893

Figure 1: Photo of the device in the basin

(U), peak wave period (Tp) and significant wave height (Hs) data. The joint distribution fitting method followed Li, Gao, & Moan (2013) using U as the marginal distribution, then $Hs|U$ then $Tp|Hs|U$. The sea state taken as the extreme in parked conditions was that with maximum Hs shown in figure 2. It is worth noting that this extreme sea state is significantly different to that which would be identified if only using Hs and Tp. In (Li, Gao, & Moan 2013) they give the extreme Hs for the Wave Hub site off Cornwall calculated from the marginal Hs distribution and from the 3 parameter distribution and the value for the latter was 37% larger. The fitting of joint distributions and the selection of an extreme sea state along a return period contour is no easy task and there are several projects which have tried to tackle this problem in recent years e.g. ESCADES (Ross et al. 2020)

Table 2: Locations of model and probes. x is given as distance from the wave paddles.

Position	Model	Probe 1	Probe 2	Probe 3
$x(m)$	17.3	7.3	9.8	17.3
$y(m)$	0	0	0	-1.5

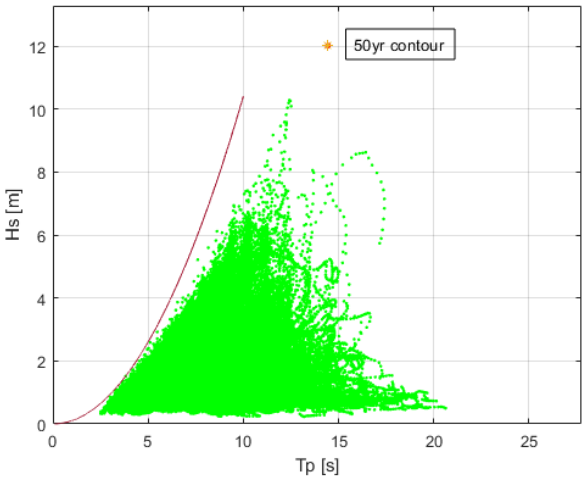

Figure 2: Sea states chosen for study with 1hr hindcast data points under layed in green. The line shows the theoretical steepness limit and the extreme sea state at the peak of the 50yr return contour is shown.

and 'improved models for multivariate metocean extremes' (IMEX) (de Hauteclocque et al. 2021). This however is not the focus of this paper as it is the comparison of the characteristic load predictions from irregular compared to constrained focused wave methods within the design sea state which is of interest. Therefore a sea state is selected following (Li, Gao, & Moan 2013) using U, Hs, Tp with the recognition that this step in the design process is a significant source of uncertainty and the sea state used has a significantly larger return period than the target. The extreme sea state selected at the peak of the contour is shown in figure 2.

5 RESULTS AND DISCUSSION

18 irregular wave seeds were run for the 50yr contour sea state, the RAOs calculated and constrained focused waves produced to compare the characteristic load predictions for the responses of interest. The focused waves were constrained so that the extreme responses occur at a target time of $50s$ e.g. $50s$ of preceding wave is simulated including $7s$ of paddle ramp time and inactivity. The positive pitch direction is defined as being in line with the wave direction i.e. a negative value occurs when the FOWT pitches into the oncoming waves. The response spectra are plotted in figure 3 and show the significant low frequency contributions to pitch and the mooring load responses. The low frequency contribution around approximately $0.05Hz$ is caused by the low frequency surge motion. These low frequency motions of semi-subs have been the subject of much study in recent years as the majority of numerical models have failed to replicate them (Robertson et al. (2020), Robertson & Wang (2021)). For surge and therefore the mooring load, this was found to be due to so called viscous drift (Ma et al. 2020) which is a third order effect due to drag (Wang et al. 2022), primarily above the mean

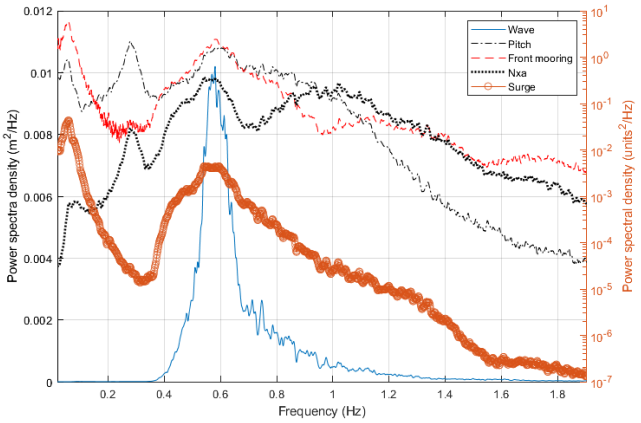

Figure 3: Spectral density plots for the responses of interest in the 50yr contour sea state. The wave spectral density magnitude is given by the left y axis while a log scale is used for the response spectra on the right y axis.

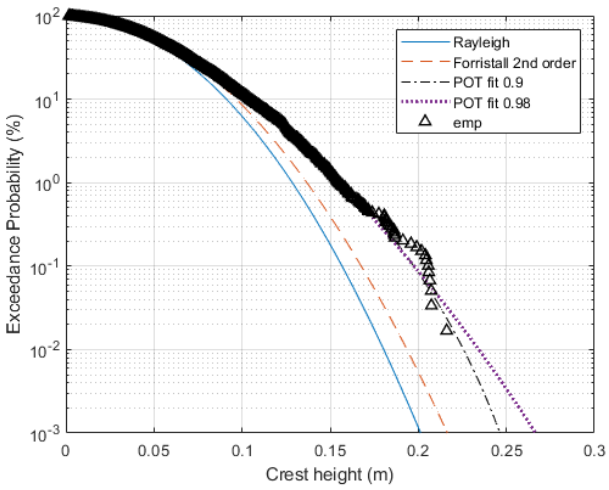

Figure 4: Exceedance plots of the wave amplitude distribution for 18 seeds. The triangles show the empirical EVD of the peaks from the irregular waves which the POT fit is predicted from. Hs values are given as full scale (model scale). 2 threshold values are shown to highlight the uncertainty in the result due to threshold selection.

still water level. This response therefore will be most significant for the largest waves and will not necessarily follow the same wave profile leading to the extreme response as the linear RAOs would predict for the MLER wave.

Figure 4 demonstrates how the extreme wave amplitude distribution significantly deviates from both linear and second order theory. This is one reason for scaling the focused waves to a high percentile of the linear EVD.

As there are significant nonlinear contributions to the pitch and mooring load responses it is important to compare the response conditioned focused waves to the true profiles observed which lead to extreme responses during irregular wave runs. The wave profile leading to the pitch maxima from each of the 18 irregular wave runs can be seen in figure 5 along with pitch response, surge position and their means. It can be seen that a mean profile is observable in both the wave profile and pitch response it leads to.

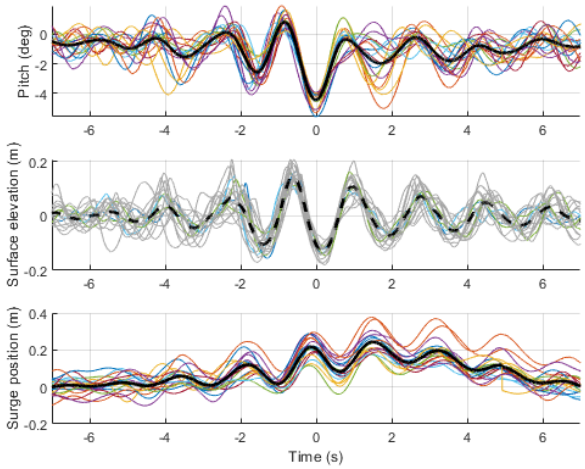

Figure 5: Profiles of surface elevation, surge position and pitch leading to the single largest negative pitch response in a 1 hour exposure time for the 18 irregular wave seeds. Averages of the extremes are given by the thick lines. The extreme response occurs at 0 seconds.

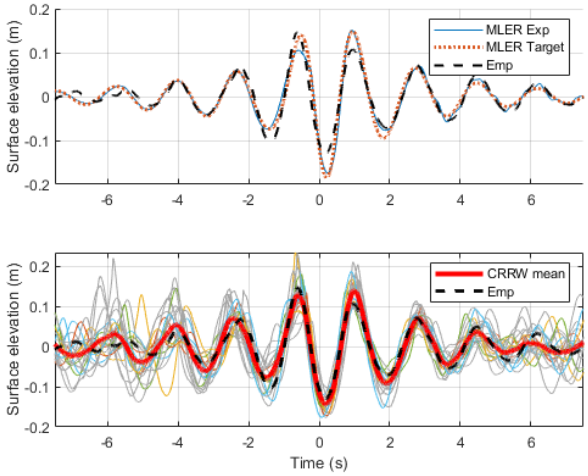

Figure 6: Comparison of the negative pitch MLER theoretical target and physically achieved (after a single phase correction) profiles to the empirical mean of the 18 profiles leading to the single largest response in a 1 hour exposure time for the 18 irregular wave seeds. The same comparison for the 20 CRRWs is also shown as measured in the physical experiments.

The MLER and CRRW profiles are presented in figure 6 along with the empirical wave profile from figure 5. There is reasonable agreement between the mean profile of the CRRWs and the empirical mean despite the contributions to the response outside of the wave frequencies.

The pitch responses produced by the CRRWs are indicated by the vertical dotted lines in figure 7, the maxima by dashed lines and the MLER by the filled line. The mean response from the 20 CRRWs and irregular wave maxima are given by thicker lines of their respective line styles. The CDF of the short term EVD is also shown and it can be seen that the MLER gives a response in line with the mean of the irregular wave maxima (thick dashed line) and the CRRW mean (thick dotted line) is slightly larger than both. It is recommended in the fixed offshore wind standards (IEC (2014), DNV (2016)) that a minimum of 6 val-

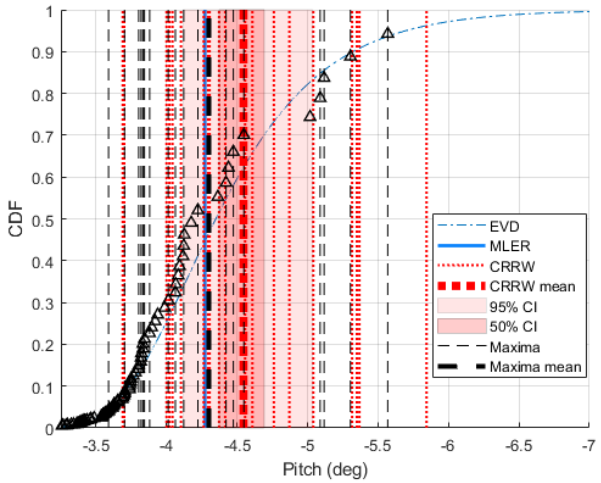

Figure 7: EVD of the negative pitch, the shading shows the 50 and 95% confidence intervals of the mean of 6 CRRWs based on a bootstrapping method using 10000 samples. The triangles show the empirical EVD of the peaks from the irregular waves which the EVD is predicted from. The dashed lines labelled maxima show the largest response from each of the 18 irregular wave seeds.

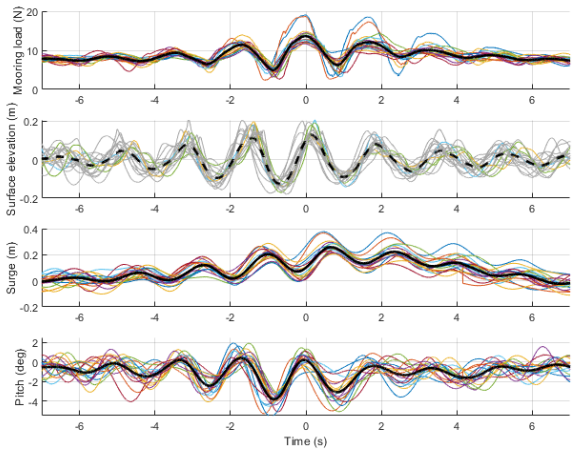

Figure 8: 18 profiles of surface elevation, surge position and pitch leading to the single largest front mooring load response in a 1 hour exposure time for the 18 irregular wave seeds. Averages of the extremes are given by the thick lines and the extreme response occurs at 0 seconds.

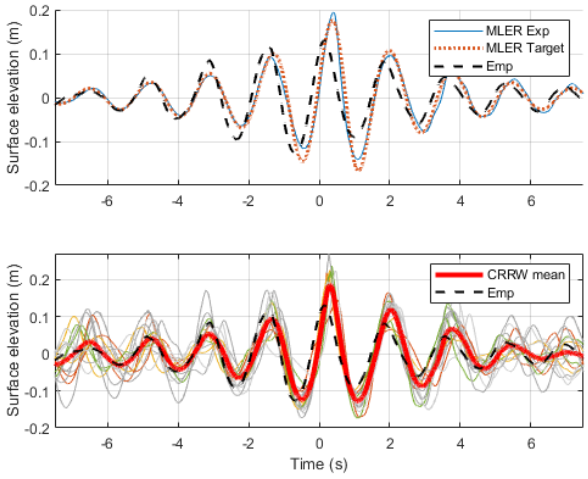

Figure 9: Comparison of the front mooring load MLER theoretical target and physically achieved (after a single phase correction) profiles to the empirical average of the 18 profiles leading to the single largest response in a 1 hour exposure time for the 18 seeds.

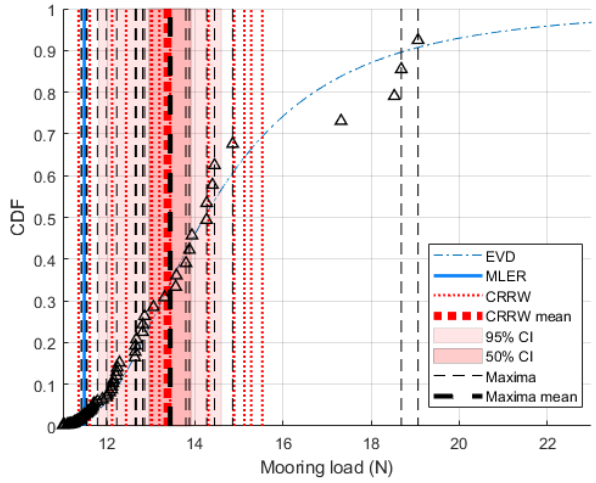

Figure 10: EVD of the front mooring load, the shading shows the 50 and 95% confidence intervals. The triangles show the empirical EVD of the peaks from the irregular waves which the EVD is predicted from. 20 CRRW responses are shown. The dashed lines labelled maxima show the largest response from each of the 18 irregular wave seeds.

ues be used in averaging and so a generalised extreme value (GEV) distribution is fit to the 20 CRRW responses and the mean of a random sample of 6 values is then calculated 10000 times to give bootstrapped confidence intervals (CIs). The 50% CIs are given by the dark background shading and 95% by the lighter shading. The peaks from all the irregular waves which the EVD is estimated from are indicated by the empirical distribution given by the triangle markers, this is done using a peak over threshold method with the threshold set to the 90th percentile of the peaks.

The extreme front mooring load appears to be caused by a sequence of 2 large waves as shown in figure 8.

The empirical profile leading to the extreme mooring load does not match the MLER profile in figure 9. This is potentially due to the significance of the low frequency component of the response caused by drag. Constraining the shape of a wave group resulting in two large crests will likely better replicate the extreme responses and will be the subject of future work.

Despite the MLER and empirical profiles not being in agreement, the characteristic load estimates are very similar as indicated by the proximity of the thick vertical lines in figure 10, but they do not produce any loads above the 70th percentile of the EVD. In this instance the MLER wave did not produce a mooring load near the characteristic load which is to be expected as the surge position makes a significant contribution and is influenced by the preceding wave.

The x and z components of the nacelle acceleration are often taken as responses of interest for FOWTs as they are restricted by the turbine manufacturer. Vigara et al. (2019) define the design basis for 2 different floating wind platform concepts both utilising the IEA 15MW turbine and offer some initial ranges for

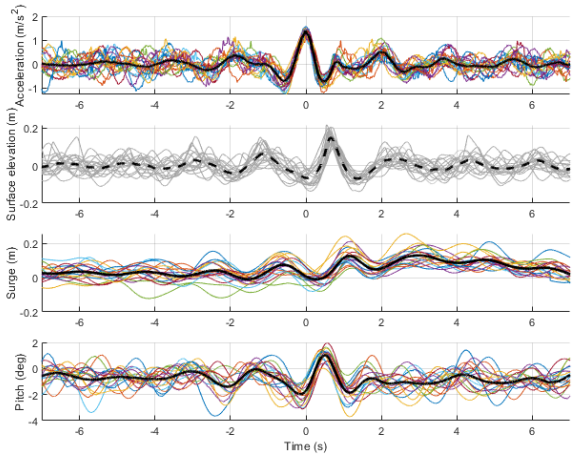

Figure 11: 18 profiles of surface elevation, surge position and pitch leading to the single largest nacelle x acceleration response in a 1 hour exposure time for the 18 irregular wave seeds. Averages of the extremes are given by the thick lines and the extreme response occurs at 0 seconds.

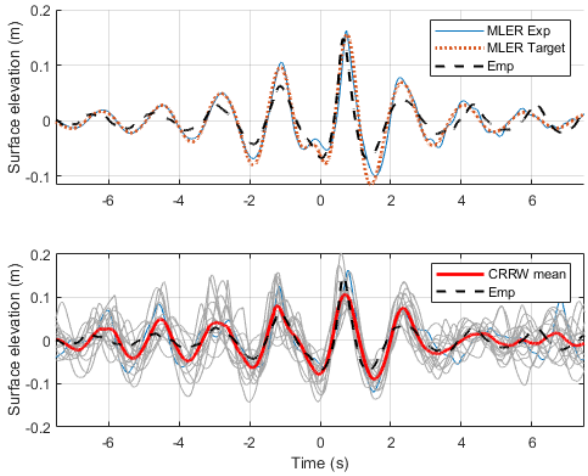

Figure 12: Comparison of the nacelle x acceleration MLER theoretical target and physically achieved (after a single phase correction) profiles to the empirical average of the 18 profiles leading to the single largest response in a 1 hour exposure time for the 18 seeds.

permissible device motions. The x component of the acceleration was selected for study using constrained waves and it can be seen in figure 12 that the MLER and empirical profiles match well.

Figure 11 shows that it is a change in the direction of the pitch response which most significantly influences the nacelle acceleration.

Figure 13 demonstrates that the MLER wave produces a response at a high percentile above the characteristic response prediction from the irregular waves. The mean of the CRRW responses is slightly below the irregular wave mean and shows that for some response types a single focused ave (MLER in this instance) may produce larger responses than the average of the constrained version.

The back mooring load is another such response where the MLER produces a larger estimate than the mean of the CRRWs as seen in figure 16. Although all the waves studied here are unidirectional and head on

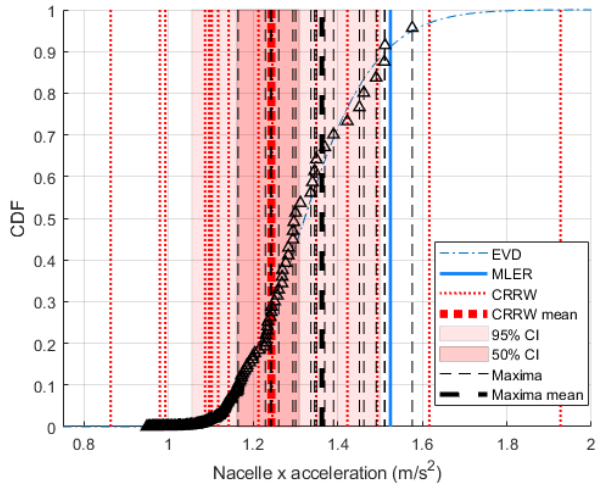

Figure 13: EVD of the nacelle x acceleration, the shading shows the 50 and 95% confidence intervals. 15 CRRW responses are shown. The triangles show the empirical EVD of the peaks from the irregular waves which the EVD is predicted from. The dashed lines labelled maxima show the largest response from each of the 18 irregular wave seeds.

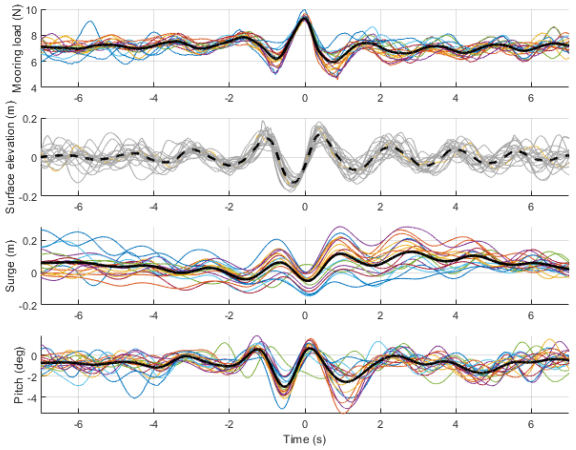

Figure 14: 18 profiles of surface elevation, surge position and pitch leading to the single largest back mooring load response in a 1 hour exposure time for the 18 seeds. Averages of the extremes are given by the thick lines and the extreme response occurs at 0 seconds.

the back mooring load will most likely be at a maximum for a sea state with a different mean wave direction and with directional spreading, it is studied here regardless as being representative of a category of response where the extreme will occur during a small surge offset as shown in figure 14.

The characteristic load estimates are given in tables 3-4 as percentiles and absolute values. The value at the 95th percentile is also reported though not for the mooring load where both IEC and DNV standards use the average of maxima approach. For the front mooring load the characteristic value predictions from the IWs and CRRWs are within 0.06N of one another though as discussed previously this is something of a coincidence and was not observed to be the case for other sea states. Judged against the irregular waves, both the MLER and CRRW methods produced reasonable characteristic load predictions in pitch. The

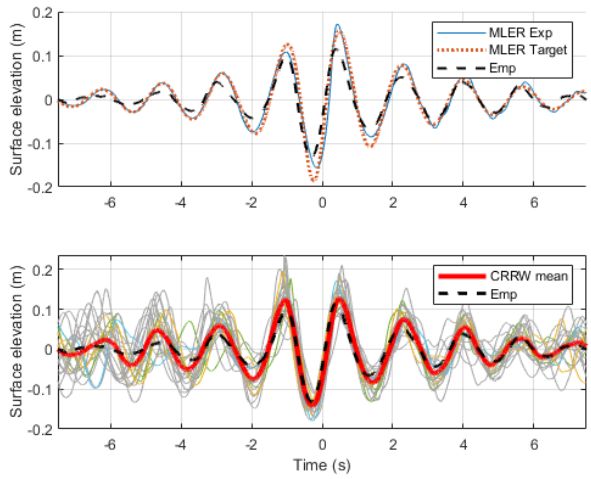

Figure 15: Comparison of the back mooring load MLER theoretical target and physically achieved (after a single phase correction) profiles to the empirical average of the 18 profiles leading to the single largest response in a 1 hour exposure time for the 18 seeds.

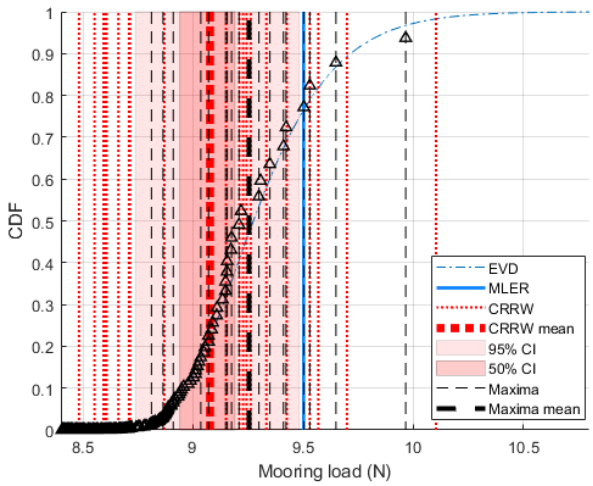

Figure 16: EVD of the back mooring load, the red shading shows the 50 and 95% confidence intervals. 15 CRRW responses are shown. The triangles show the empirical EVD of the peaks from the irregular waves which the EVD is predicted from. The dashed lines labelled maxima show the largest response from each of the 18 irregular wave seeds.

back mooring load and nacelle acceleration in x produced similar comparisons between the relative values from MLER, CRRW and irregular wave characteristic load predictions as evidenced in figures 13-16.

6 CONCLUSIONS

A procedure for characteristic load prediction using constrained focused waves developed as part of work package 4 of the Supergen ORE Hub was applied during physical model testing to a semi-sub FOWT. The results suggest that when applying an appropriate wave calibration and scaling the waves to a large percentile of the linearly predicted target response distribution, short design waves can produce characteristic load estimates in line with irregular wave methods in a shorter time. These time savings are greater when a 3 hour exposure time is used and the focused and constrained focused waves are short enough that high fidelity models, such as computational fluid dynamics may be used. For the pitch dominated responses in the sea state studied, a single focused wave may be enough but for responses where a large surge position is important constrained waves are required. Whilst the CRRWs for the front mooring load were able to produce a characteristic load prediction in line with the irregular waves, the mean profile was significantly different to the empirical one. This is not found to always be the case however; for the sea state producing the extreme front mooring load for constant wind loading on the rated wind speed contour the CRRWs failed to produce an extreme in line with the irregular waves and the MLER profile was significantly different to the empirical one. These results are not shown here but will be investigated in a subsequent paper with the aid of a numerical model.

It should be emphasised again that for steeper sea states constrained wave methods will be more difficult to implement due to wave breaking. Doubt has also been cast on the applicability of a contour approach for FOWTs due to the importance of wind loading (Li, Gao, & Moan 2013), (DNV 2018). Future work will investigate the method applied to a contour at the rated wind speed under operational conditions and the suitability of constrained waves to improve the efficiency of other characteristic load prediction methods.

7 ACKNOWLEDGEMENTS

This work was supported by the Engineering and Physical Sciences Research Council (EPSRC, reference EP/S000747/1) through the Supergen ORE Hub.

Table 3: Characteristic load prediction comparisons. FM = front mooring, P = Pitch. FM($\%$) refers to the percentile of the EVD CDF, FM(N) the magnitude. $95th$ refers to the magnitude of the response at the $95th$ percentile of the EVD CDF.

Wave type	FM ($\%$)	FM (N)	P ($\%$)	P (deg)	P $95th(deg)$
IW	34.3	13.44	48.2	-4.30	-5.70
MLER	1.4	11.49	46.2	-4.27	-
CRRW	33.0	13.38	63.7	-4.55	-

Table 4: Characteristic load prediction comparisons. BM = back mooring, Nxa = nacelle x acceleration. BM($\%$) refers to the percentile of the EVD CDF, BM(N) the magnitude. $95th$ refers to the magnitude of the response at the $95th$ percentile of the EVD CDF.

Wave type	BM ($\%$)	BM (N)	BM $95th(N)$	Nxa ($\%$)	Nxa (m/s^2)	Nxa $95th(m/s^2)$
IW	47.5	9.26	9.87	62.0	1.35	1.58
MLER	76.6	9.50	-	91.1	1.52	-
CRRW	22.2	9.08	-	25.5	1.24	-

REFERENCES

Allen, C., A. Viscelli, H. Dagher, A. Goupee, E. Gaertner, N. Abbas, M. Hall, & G. Barter (2020). Definition of the umaine volturnus-s reference platform developed for the iea wind 15-megawatt offshore reference wind turbine. Technical report, National Renewable Energy Lab.(NREL), Golden, CO (United States).

de Hauteclocque, G., E. Mackay, & E. Vanem (2021). Quantitative assessment of environmental contour approaches (preprint from march 2021).

Dietz, J. S. (2005). *Application of conditional waves as critical wave episodes for extreme loads on marine structures*. Technical University of Denmark.

DNV (2014a). Environmental conditions and environmental loads. *Recommend Practice DNV-RP-C205 182*.

DNV (2014b). Environmental conditions and environmental loads. *Høvik, Norway: DNV GL. Available at: https://rules. dnvgl. com/docs/pdf/DNV/codes/docs/2014-04/RP-C205. pdf. Accessed March 15*, 2018.

DNV (2015). Offshore standard dnvgl-os-e301 position mooring. *Høvik, DNV GL AS.[Online] Available from: https://rules. dnvgl. com/docs/pdf/dnvgl/os/2015-07/DNVGLOS-E301. pdf [Accessed 5th February 2018]*.

DNV (2016). Loads and site conditions for wind turbines.

DNV (2018). Dnvgl-st-0119: Floating wind turbine structures. *DNV GL*.

Hersbach, H., B. Bell, P. Berrisford, G. Biavati, A. Horányi, J. Muñoz Sabater, J. Nicolas, C. Peubey, R. Radu, I. Rozum, et al. (2018). Era5 hourly data on single levels from 1979 to present. *Copernicus Climate Change Service (C3S) Climate Data Store (CDS) 10*.

IEC (2014). Iec 61400-3-1, wind turbines-part 3-1: Design requirements for offshore wind turbines, committee draft. sl: Iec, 2014. Technical report.

IEC (2015). Iec ts 62600-10: Marine energy—wave, tidal and other water current converters.

IEC (2016). 62600-2. 2016. marine energy-wave, tidal and other water current converters-part 2: design requirements for marine energy systems.

IEC (2019). Iec 61400-3-2 wind energy generation systems-part 3-2: Design requirements for floating offshore wind turbines.

Li, L., Z. Gao, & T. Moan (2013). Joint environmental data at five european offshore sites for design of combined wind and wave energy devices. In *International Conference on Offshore Mechanics and Arctic Engineering*, Volume 55423, pp. V008T09A006. American Society of Mechanical Engineers.

Ma, S., D.-k. Xu, W.-y. Duan, J.-k. Chen, K.-p. Liao, & H. Wang (2020). The numerical study of viscous drag force influence on low-frequency surge motion of a semi-submersible in storm sea states. *Ocean Engineering 213*, 107511.

Quon, E., A. Platt, Y.-H. Yu, & M. Lawson (2016). Application of the most likely extreme response method for wave energy converters. In *ASME 2016 35th International Conference on Ocean, Offshore and Arctic Engineering*. American Society of Mechanical Engineers Digital Collection.

Rainey, P. & T. Camp (2007). Constrained non-linear waves for offshore wind turbine design. In *Journal of Physics: Conference Series*, Volume 75, pp. 012067. IOP Publishing.

Robertson, A. & L. Wang (2021). Oc6 phase ib: Floating wind component experiment for difference-frequency hydrodynamic load validation. *Energies 14*(19), 6417.

Robertson, A. N., S. Gueydon, E. Bachynski, L. Wang, J. Jonkman, D. Alarcón, E. Amet, A. Beardsell, P. Bonnet, B. Boudet, et al. (2020). Oc6 phase i: Investigating the underprediction of low-frequency hydrodynamic loads and responses of a floating wind turbine. In *Journal of Physics: Conference Series*, Volume 1618, pp. 032033. IOP Publishing.

Ross, E., O. C. Astrup, E. Bitner-Gregersen, N. Bunn, G. Feld, B. Gouldby, A. Huseby, Y. Liu, D. Randell, E. Vanem, et al. (2020). On environmental contours for marine and coastal design. *Ocean Engineering 195*, 106194.

Tosdevin, T., S. Jin, A. Cao, D. Simmonds, M. Hann, , & D. Greaves (2021). Extreme responses of a hinged raft type wave energy convertor.

Tromans, P. S., A. R. Anaturk, P. Hagemeijer, et al. (1991). A new model for the kinematics of large ocean waves-application as a design wave. In *The first international offshore and polar engineering conference*. International Society of Offshore and Polar Engineers.

Vigara, F., L. Cerdán, R. Durán, S. Muñoz, M. Lynch, S. Doole, et al. (2019). Corewind d1. 2: Design load basis.

Viselli, A. M., G. Z. Forristall, B. R. Pearce, & H. J. Dagher (2015). Estimation of extreme wave and wind design parameters for offshore wind turbines in the gulf of maine using a pot method. *Ocean Engineering 104*, 649–658.

Wang, L., A. Robertson, J. Jonkman, & Y.-H. Yu (2022). Oc6 phase i: Improvements to the openfast predictions of nonlinear, low-frequency responses of a floating offshore wind turbine platform. *Renewable Energy*.

Winterstein, S. R., T. C. Ude, C. A. Cornell, P. Bjerager, & S. Haver (1993). Environmental parameters for extreme response: Inverse form with omission factors. In *Proc. 6th Int. Conf. on Structural Safety and Reliability, Innsbruck, Austria*.